



CHORUS

This is the accepted manuscript made available via CHORUS. The article has been published as:

Phase diagram of the $J_{\{1\}}-J_{\{2\}}-J_{\{3\}}$ Heisenberg model on the honeycomb lattice: A series expansion study

J. Oitmaa and R. R. P. Singh

Phys. Rev. B **84**, 094424 — Published 20 September 2011

DOI: [10.1103/PhysRevB.84.094424](https://doi.org/10.1103/PhysRevB.84.094424)

Phase Diagram of the J_1, J_2, J_3 Heisenberg Models on the Honeycomb Lattice: A Series Expansion Study

J. Oitmaa

School of Physics, The University of New South Wales, Sydney 2052, Australia

R. R. P. Singh

University of California Davis, CA 95616, USA

(Dated: August 24, 2011)

We study magnetically ordered phases and their phase boundaries in the $J_1 - J_2 - J_3$ Heisenberg models on the honeycomb lattice using series expansions around Néel and different collinear and non-collinear magnetic states. An Ising anisotropy ($\lambda = J_\perp/J_z \neq 1$) is introduced and ground state energy and magnetization order parameter are calculated as a power series expansion in λ . Series extrapolation methods are used to study properties for the Heisenberg model ($\lambda = 1$). We find that at large J_3 (> 0.6) there is a first order transition between Néel and columnar states, in agreement with the classical answer. For $J_3 = 0$, we find that the Néel phase extends beyond the region of classical stability. We also find that spiral phases are stabilized over large parameter regions, although their spiral angles can be substantially renormalized with respect to the classical values. Our study also shows a magnetically disordered region at intermediate J_2/J_1 and J_3/J_1 values.

PACS numbers: 74.70.-b, 75.10.Jm, 75.40.Gb, 75.30.Ds

I. INTRODUCTION

The search for quantum spin-liquid phases in realistic spin and electronic models and real materials remains a very active area of research. In recent years a number of experimental materials have been synthesized, whose behavior has been very promising from the point of view of discovering such a phase. These include many kagome and triangular lattice based frustrated magnets.¹⁻⁴ In several cases, the frustration parameter,⁵ defined as the ratio of the Curie-Weiss temperature to any magnetic ordering temperature exceeds 1000. Most of these experimental systems show gapless spin excitations, though the role of impurities and weak anisotropies in creating gapless spin excitations has not been ruled out.

From a theoretical point of view, frustration is essential for obtaining a spin-liquid phase in dimensions greater than one. Unfrustrated two-dimensional spin models show robust Néel order. However, both spin-frustration arising from competing exchange interactions and frustration arising from the itineracy of the electrons can lead to a spin-liquid phase. In recent years several realistic models have emerged as candidates for quantum spin-liquid ground states. One is the Heisenberg model on a kagome lattice, where extensive Density Matrix Renormalization Group work by Yan et al⁶ presents strong evidence for a spin-liquid phase with a not-too-small gap to singlet and triplet excitations. Another is the triangular-lattice antiferromagnet with Heisenberg and 4-spin ring exchanges.^{7,8} A third, somewhat unexpected case, is the half-filled honeycomb lattice Hubbard model,⁹ which would lead to an unfrustrated Heisenberg model at large U . It shows a spin-liquid phase at intermediate values of U , sandwiched between a Néel phase at large U and a semi-metal phase at small U .¹⁰ This spin-liquid phase was also found to be gapped with no

signs of any broken symmetry.

The question of whether this latter phase can be realized in a frustrated spin model on the honeycomb lattice, arising from higher order charge exchange processes has attracted considerable interest.¹¹ Several recent papers have investigated this question using exact diagonalization, Schwinger-Boson and spin-wave theory, coupled cluster methods, and variational wavefunctions. They have come to conflicting conclusions about the phase diagram and the possible existence of a spin-liquid phase in this model.¹²⁻¹⁸ Experimental realizations of spin-half honeycomb lattice Heisenberg model have been discussed recently by Tsirlin et al.¹⁹

Here we study the phase diagram of frustrated Heisenberg model on the honeycomb lattice using series expansions.^{20,21} We will confine our study to all exchanges being positive ($J_1, J_2, J_3 > 0$) (See Fig. 1). The nearest-neighbor honeycomb lattice Heisenberg model, with antiferromagnetic exchange J_1 (which we set to unity), is well known to have a Néel ordered ground state.²²⁻²⁸ Adding a frustrating second neighbor antiferromagnetic interaction J_2 and a third neighbor antiferromagnetic interaction J_3 leads to a complex phase diagram even at a classical level^{26,28} that includes Néel, columnar and different spiral phases (See Fig. 2). We have carried out series expansions around Néel, columnar and spiral phases. For large J_3 (> 0.6) we find a direct first order transition between Néel and columnar phases as a function of J_2 . Thus, the most interesting part of the phase diagram is for $J_3 < 0.6$. We have studied this phase diagram along constant J_3 lines as a function of J_2 as well as along the contour $J_3 = J_2$. We find that at small J_3 the Néel phase widens due to quantum fluctuations, in agreement with recent exact diagonalization study.¹⁸ We also find that spiral phases are stabilized for intermediate and large J_2 . The spiral angles are strongly renormalized

with respect to their classical values. However, they do not lock into commensurate colinear structures as suggested in recent exact diagonalization study.¹⁸ Rather, our studies favor angles closer to 90 degrees, which implies spins pointing at right angles.

Our study also shows that a part of the phase diagram at small and intermediate J_3 and J_2 has no magnetic long range order. The convergence of our series expansion is best for colinear phases, when they have clearly non-zero order parameters. We are unable to accurately obtain the region of stability of magnetically disordered phases, but it is clear from the general analysis that such a phase must exist. This is also clearly seen by going along $J_2 = J_3$, where such a phase exists near the highly frustrated point $J_2 = J_3 = 0.5$.¹³ It is possible that a strip of this phase extends all the way down to $J_3 = 0$.

In order to gain some insight into the nature of this phase, we have also carried out series expansions around a dimer state, which was considered as a possible ground state in Ref. 12. Following Moessner et al,²⁹ such a dimer state is called a staggered dimer state. However, we found that the staggered dimer phase has rather high energy and thus is not stabilized for $J_3 = 0$. While our study can not rule out such a phase for $J_3 = 0.3$ and intermediate J_2 , the energies again suggest that the staggered dimer state has too high an energy. This should be contrasted with studies of the square-lattice $J_1 - J_2$ models, where energies of dimer-phases match smoothly with the magnetically ordered phases at intermediate J_2/J_1 values.³⁰ It is possible that some other dimer or plaquette phase is stable here.¹⁸ Investigation of larger unit cell Dimer/Plaquette phases is left for future work.

II. MODELS AND SERIES EXPANSIONS

We study the honeycomb-lattice Heisenberg model with Hamiltonian

$$\mathcal{H} = J_1 \sum_{\langle i,j \rangle} \vec{S}_i \cdot \vec{S}_j + J_2 \sum_{(i,k)} \vec{S}_i \cdot \vec{S}_k + J_3 \sum_{[i,l]} \vec{S}_i \cdot \vec{S}_l. \quad (1)$$

The exchanges within an elementary hexagon are shown in Fig. 1. Without loss of generality, we take $J_1 = 1$. The classical phase diagram for $J_2 > 0$, $J_3 > 0$ is sketched in Fig. 2. The spin structure of the classical phases are shown in Fig. 3. It consists of the Néel phase, a columnar phases, which is also colinear, and two planar spiral phases. In the spiral-I phase the pitch vector \vec{Q} is perpendicular to one of the bond directions, and is characterized by a single angle θ . Spins twist away from the Néel state by this angle as one goes from one row to the next. In the spiral-II phase the pitch vector is parallel to one of the bond directions. It is characterized by two angles, θ and ϕ . Within a unit cell, the spins deviate from the Néel state by an angle ϕ . In addition, there is a twist by an angle θ as one goes from one unit cell to next. The spiral II phase is stabilized by negative J_3 but becomes degenerate with the spiral I phase for $J_3 = 0$ and

$1/6 < J_2 < 1/2$. Also, at $J_2 = 1/2$, the spiral-II phase locks into another colinear phase with $\phi = \pi$, $\theta = \pi$.

To carry out an Ising expansion around a colinear state (Néel or columnar), we introduce an Ising anisotropy in all the exchange interactions,

$$\vec{S}_i \cdot \vec{S}_j = S_i^z S_j^z + \lambda(S_i^x S_j^x + S_i^y S_j^y). \quad (2)$$

We calculate series expansions in the variable λ for the ground state energy, per spin, e_0 and the sublattice magnetization m .

The reader unfamiliar with series expansion methods can find technical details in Refs. 20,21 and we shall not elaborate here. However it is worth mentioning that it is convenient, for both colinear and non-colinear states, to rotate the spin axes on different sites to give an unperturbed ground state in which all spins are aligned. This procedure has been described in ref. 32. This transformation has the effect of complicating the form of the Hamiltonian but avoids the need to identify sublattice types in the cluster data.

To derive series to a given order n requires enumeration of clusters with up to n sites. This number grows rapidly with n , and this is the major factor limiting the length of series. For example, for the 8th order series for the spiral I phase for the full J1-J2-J3 model a total of 1,083,315 distinct clusters occur. For the J1-J2 model an additional term can be obtained, requiring a total of 1,172,204 clusters.

The spiral II phase is only considered for $J_3 = 0$ (it is not stabilized classically for positive J_3). It has 7 bond-types and took 108,453 distinct clusters to calculate the series to 8th order. For both the spiral phases, we allow angles (such as θ , ϕ) different from classical values and take the angles that minimize the ground state energy.

In addition, we have also developed series expansion for the ground state energy of the dimer configuration shown in Fig. 4. The center of the dimers form a triangular-lattice with three different types of inter-dimer interactions with J_1 , J_2 and J_3 all non-zero. To carry out the calculation to 8-th order required 33826 linked clusters.

The series data is too lengthy to reproduce here, but can be provided on request. The data for selected values of the exchange parameters are provided in the Supplemental Material.³³

III. SERIES ANALYSIS AND RESULTS

We will restrict attention to a few contours in the $J_2 - J_3$ plane. We will consider $J_3 = 0$, $J_3 = 0.3$, $J_3 = 0.6$ and $J_3 = 1$, and $J_3 = J_2$. For large J_3 Néel and columnar states are considered, whereas for small J_3 Néel and spiral phases are considered.

The series are analyzed by Padé as well as d-log Padé approximants. These approximants are constructed in the variable λ as well as in the variable $\delta = 2\lambda - \lambda^2$. The latter³⁴ allows one to eliminate a square-root singularity due to the gapless spin-waves at $\lambda = 1$.

In Fig. 5, we show the ground state energy of the Néel and columnar phases for different values of J_3 . The corresponding magnetizations are shown in Fig. 6. For $J_3 = 1.0$, there is a clear first order phase transition between the Néel and columnar phases around $J_2 > 0.5$. An estimate of the transition point can be obtained by the linear fits to the energy data (also shown). For $J_3 = 0.6$, the transition from the two sides is close to becoming continuous. The order parameters for both phases approach zero as J_2 approaches 0.5. Very near the transition, the series analysis is not reliable enough to tell if this is a continuous transition, or a first order transition, or there is a small intermediate region with no magnetic order, although a direct transition between the phases will necessarily be first order, as seen by the linear fits to the ground state energy.

The sharp downturn in the columnar-state magnetization for larger J_2 is a clear signature of an impending transition to the spiral I phase, which classically would occur at $J_2 = 0.7$.

In Fig. 7, we show the magnetization for the Néel and columnar phases along the contour $J_2 = J_3$ in the parameter space. We can see that both order parameters go to zero before the highly frustrated point $J_2 = J_3 = 0.5$ is reached and there is an intermediate phase with no magnetic order. This agrees with previous theoretical study by Cabra et al.¹³

At small J_3 (for example $J_3 = 0$) the region of Néel order is increased with respect to the classical answer, but that is no longer true for $J_3 = 0.3$. For $J_3 = 0$, we estimate that Néel order extends upto $J_2 = 0.20$ compared to the classical value of $1/6$. In contrast, for $J_3 = 0.3$, the magnetization vanishes near $J_2 = 0.3$ compared to the classical value of $11/30$ (See Fig. 6). We do not find any clear evidence for a magnetically disordered phase at $J_3 = 0$. Fig. 8 shows the ground state energy for Néel, spiral-I, spiral-II and staggered dimer phases for $J_3 = 0$. In the spiral phases, we consider a range of spiral angles and pick that value which minimizes the energy. In general, these energy functions are quite shallow, so that the renormalized spiral angles shown in Table-I should be considered as approximate. While the convergence is not excellent at intermediate J_2/J_1 values, our analysis suggests that one transitions from Néel to spiral-II to spiral-I phase. The staggered dimer phase is clearly not stabilized here in contrast to recent suggestions from bond-operator formalism¹² based studies. In addition, the spiral-II phase also does not lock into a collinear configuration in contrast to the conclusions from the finite-size study.¹⁸ If anything, our estimates suggest spiral angles close to 90 degrees, which implies some spins pointing at right angles with respect to their neighbors.

In Fig. 9, we show the ground state energy for Néel, spiral-I, and staggered dimer configurations along $J_3 = 0.3$, as a function of J_2 . At intermediate J_2 values the convergence of both Néel and spiral-I phases becomes poor. The energy of the staggered dimer phase appears well behaved. In this case, there is a much stronger case

for an intermediate phase with no magnetic order. However, the staggered dimer phase has a relatively high energy and it is not clear that it becomes the ground state of the system in this region. Since the ground state energy must vary continuously, it seems more likely that some other phase not considered by us becomes the ground state in this region. At large J_2 , the energy of spiral and staggered dimer phases become nearly degenerate. Our results are consistent with the suggestion from the exact diagonalization study¹⁸ that for some parameter ranges, the staggered dimer state may be difficult to distinguish from magnetically ordered states.

IV. DISCUSSIONS AND CONCLUSIONS

In this paper, we have used series expansion methods to study the ground state phase diagram of the $J_1 - J_2 - J_3$ antiferromagnetic Heisenberg models on the honeycomb lattice. We have determined the stability of Néel, columnar and various spiral phases and calculated their properties. In agreement with previous studies, we find that the region of stability of Néel phase increases with quantum fluctuations for $J_3 = 0$. However, that is not the case for larger J_3 . There clearly exists a parameter region at intermediate J_2 and J_3 with no magnetic order. This region is most clearly seen near the highly frustrated point $J_3 = J_2 = 0.5$ and possibly forms a strip extending all the way near to $J_3 = 0$. We found that the staggered dimer order is not favored for the $J_1 - J_2$ model.

The phase diagram has some resemblance to the square-lattice Heisenberg model with frustrated antiferromagnetic exchange constants. In all these systems, it remains difficult to determine the nature of the magnetically disordered phases. Our results are generally in good agreement with recent exact diagonalization study of Albuquerque et al.¹⁸ One point of difference is that we do not find that a third collinear phase (that is the spiral II with $\phi = \pi$, $\theta = \pi$) is favored over general spiral phases over any extended part of the phase diagram. This difference may be because periodic boundary conditions on finite systems may disfavor incommensurate phases. Another difference with respect to the Bond Order Mean-Field Theory study¹² is that we do not find evidence for a staggered dimer phase in the magnetically disordered region at small J_3 .

An important question is whether this magnetically disordered phase in the frustrated Heisenberg models is related to the one found by Meng et al⁹ in the Hubbard model at intermediate U/t , and whether it is a true spin-liquid. Recent work by Yang and Schmidt¹¹ found that for U/t values where Meng et al obtained a phase transition to a spin-liquid phase J_2/J_1 remains very small (of order 0.06), with J_3/J_1 even smaller. This means that just these additional interactions can not drive the transition, as our study finds that these parameters are well within the Néel phase. It is possible that larger

ring exchanges play a role in bringing about the transition. Nevertheless, the disordered phase in the Heisenberg model may be connected to the one found in the Hubbard model. This question as well as the possibility of other types of dimer/plaquette phases deserves further attention.

Acknowledgments

This work is supported in part by NSF grant number DMR-1004231.

-
- ¹ H. Fukuyama, J Phys. Soc. Jpn. 77, 111013 (2008).
² J.S. Helton et al, Phys. Rev. Lett. 98, 107204 (2007).
³ Y. Shimizu, K. Miyagawa, K. Kanoda, M. Maesato, and G. Saito, Phys. Rev. Lett. **91**, 107001 (2003).
⁴ M Yamashita et al, Science 328, 1246 (2010).
⁵ A. P. Ramirez, Ann. Rev. of Mat. Sci. 24, 453 (1994).
⁶ S. Yan, D. A. Huse and S. R. White, Science, 332, 1173 (2011).
⁷ O. I. Motrunich, Phys. Rev. B 72, 045105 (2005).
⁸ H. Y. Yang et al, Phys. Rev. Lett. 105, 267204 (2010).
⁹ Z. Y. Meng, T. C. Lang, S. Wessel, F. F. Assaad, and A. Muramatsu, Nature 464, 847 (2010).
¹⁰ T. Paiva et al, Phys. Rev. B 72, 085123 (2005).
¹¹ H. Y. Yang and K. P. Schmidt, European Physics Letters 94, 17004 (2011).
¹² A. Mulder, R. Ganesh, L. Capriotti and A. Paramekanti, Phys. Rev. B **81**, 214419 (2010).
¹³ D. C. Cabra, C. A. Lamas and H. D. Rosales, Modern Physics Letters B 83, 224406 (2011); D. C. Cabra, C. A. Lamas and H. D. Rosales, Phys. Rev. B 83, 094506 (2011).
¹⁴ B. K. Clark, D. A. Abanin and S. L. Sondhi, arXiv:1010.3011.
¹⁵ H. Mosadeq, F. Shahbazi and S. A. Jafari, J. Phys. Cond. Matt. 23, 226006 (2011).
¹⁶ D.J.J. Farnell, R.F. Bishop, P.H.Y. Li, J. Richter and C.E. Campbell, arXiv:1103.3856.
¹⁷ J. Reuther, D. Abanin and R. Thomale, arXiv:1103.0859.
¹⁸ A. F. Albuquerque, D. Schwandt, B. Hetenyi, S. Capponi, M. Mambri, and A. M. Lauchli, Phys. Rev. B 84, 024406 (2011).
¹⁹ A. A. Tsirlin, O. Janson, and H. Rosner, arXiv:1007.1646.
²⁰ J. Oitmaa, C. Hamer and W. Zheng, *Series Expansion Methods for strongly interacting lattice models* (Cambridge University Press, 2006).
²¹ M. P. Gelfand and R. R. P. Singh, Adv. Phys. **49**, 93(2000).
²² J. Oitmaa and D. D. Betts, Can. J. Phys. 56, 897 (1978).
²³ J. D. Reger, J. A. Riera and A. P. Young, J. Phys: Condensed Matter **1**, 1855 (1989).
²⁴ Z. Weihong, J. Oitmaa and C. J. Hamer, Phys. Rev. B 44, 11869 (1991).
²⁵ J. Oitmaa, C. J. Hamer and Z. Weihong, Phys. Rev. B 45, 9834 (1992).
²⁶ E. Rastelli, A. Tassi and L. Reatto, Physica 97B, 1 (1979).
²⁷ A. Mattsson, P. Frojdh and T. Einarsson, Phys. Rev. B 49, 3997 (1994); T. Einarsson and H. Johannesson Phys. Rev. B 43, 5867 (1991).
²⁸ J. B. Fouet, P. Sindzingre, and C. Lhuillier EPJ B **20**, 241 (2001).
²⁹ R. Moessner, S. L. Sondhi and P. Chandra, Phys. Rev. B 64, 144416 (2001).
³⁰ See for example, R. R. P. Singh *et al*, Phys. Rev. B 60, 7278 (1989).
³¹ R. R. P. Singh and D. A. Huse, Phys. Rev. Lett. 68, 1766-1769 (1992).
³² Zheng Weihong, R. H. Mckenzie and R. R. P. Singh, Phys. Rev. B 59, 14367 (1999).
³³ See Supplemental Material at URL
³⁴ D. A. Huse, Phys. Rev. B 37, 2380 (1988).

Figures

FIG. 1: Exchange constants of the honeycomb-lattice Heisenberg model

FIG. 2: Classical phase diagram of the honeycomb lattice Heisenberg model with $J_1 = 1$.

FIG. 3: Classical phases of the honeycomb-lattice Heisenberg model with positive J_1 , J_2 and J_3 . The phases are (a) Néel, (b) columnar, (c) spiral-I and (d) spiral-II.

FIG. 4: Staggered dimer phase on the honeycomb lattice

FIG. 5: Ground state energy estimates of the Néel phase ($J_2 < 0.5$) and the columnar phase ($J_2 > 0.5$) are shown as a function of J_2 for different values of J_3 . For $J_3 = 0.6$ and $J_3 = 1.0$ linear fits to the data points are also shown to illustrate the first order transition point between the two phases.

FIG. 6: Magnetization for Néel phase ($J_2 < 0.5$) and columnar phase ($J_2 > 0.5$) as a function of J_2 for different values of J_3 . The arrows indicate the critical J_2 values for the classical model, where the Néel order parameter vanishes, for $J_3 = 0.0$ and $J_3 = 0.3$.

FIG. 7: Order parameter for the Néel and columnar phases along $J_3 = J_2$.

FIG. 8: Ground state energy for Néel, staggered dimer, spiral-I and spiral-II phases for $J_3 = 0$.

FIG. 9: Ground state energy for Néel, staggered dimer and spiral-I phases for $J_3 = 0.3$.

Tables

Phase	J_2, J_3	θ_{cl}, ϕ_{cl}	θ_r, ϕ_r
Spiral-I	1.00, 0.0	104.5	90.0
Spiral-I	0.70, 0.0	98.2	90.0

Spiral-I	0.50, 0.0	90.0	85.0
Spiral-I	0.70, 0.3	104.5	95.0
Spiral-I	0.60, 0.3	99.6	80.0
Spiral-II	0.40, 0.0	149,125	150,95
Spiral-II	0.25, 0.0	104.5,75.5	120,80

TABLE I: Selected examples of classical spiral angles (θ_{cl} for spiral-I phase and θ_{cl} and ϕ_{cl} for spiral-II phase) and the corresponding estimated renormalized spiral angles (θ_r and ϕ_r) in degrees.

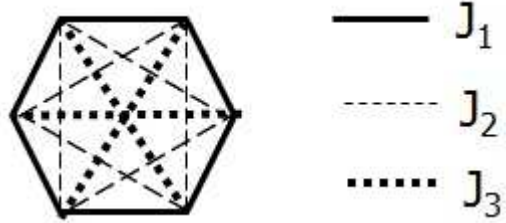


Figure 1 BG11636 24Aug2011

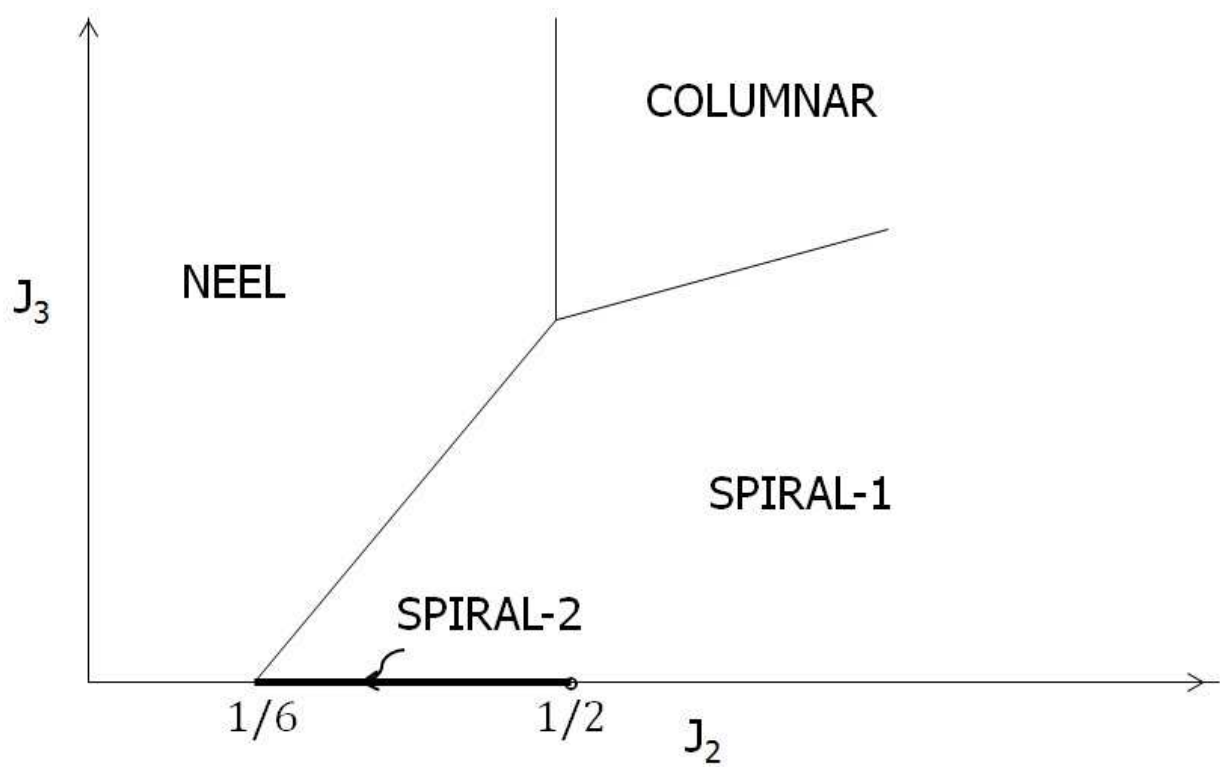


Figure 2 BG11636 24Aug2011

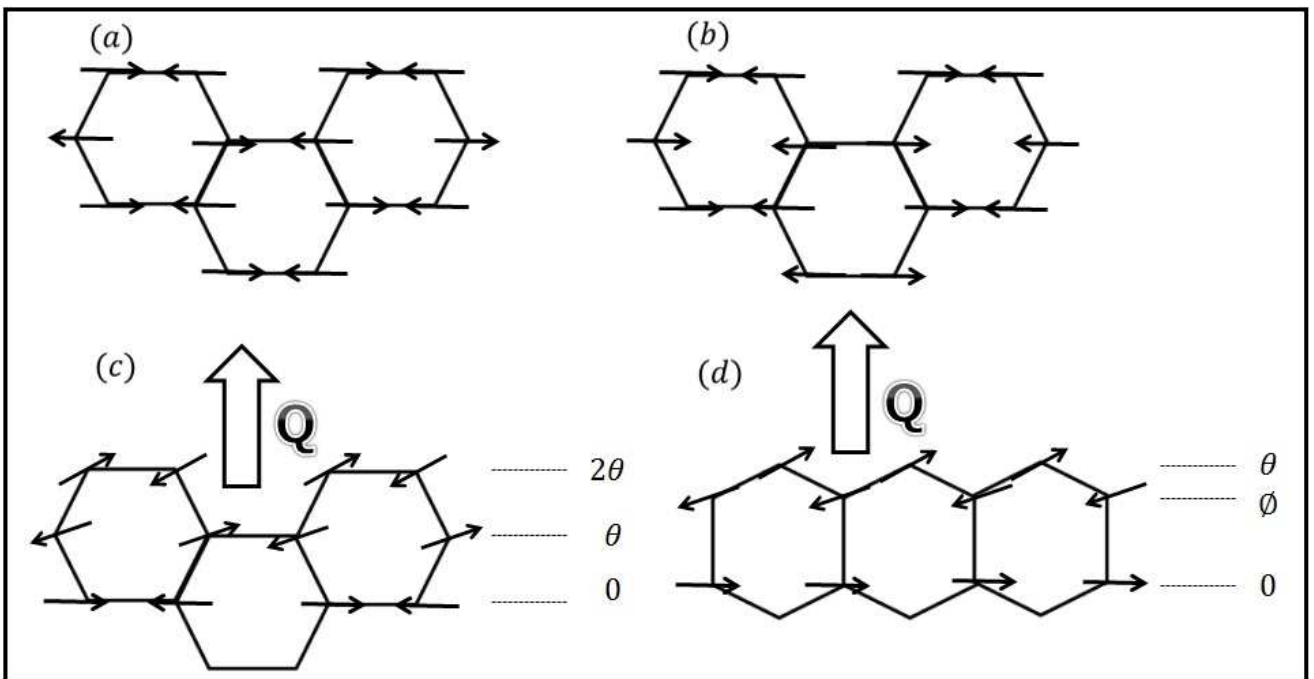


Figure 3

BG11636

24Aug2011

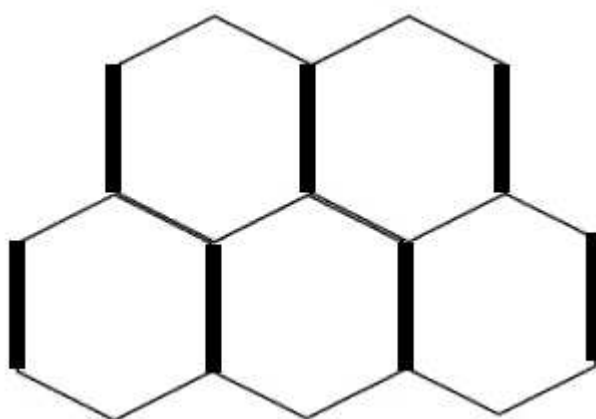


Figure 4 BG11636 24Aug2011

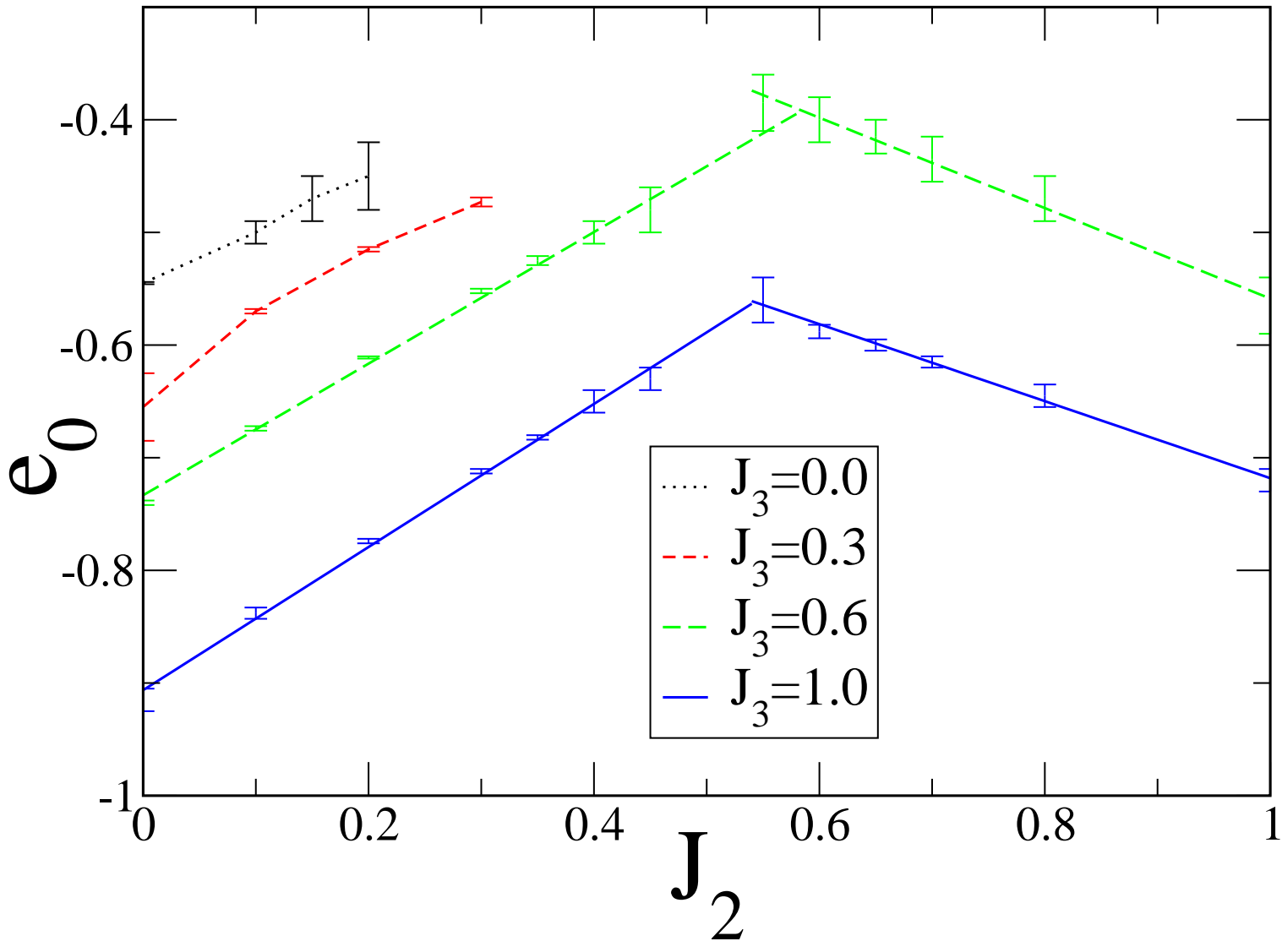


Figure 5 BG11636 24Aug2011

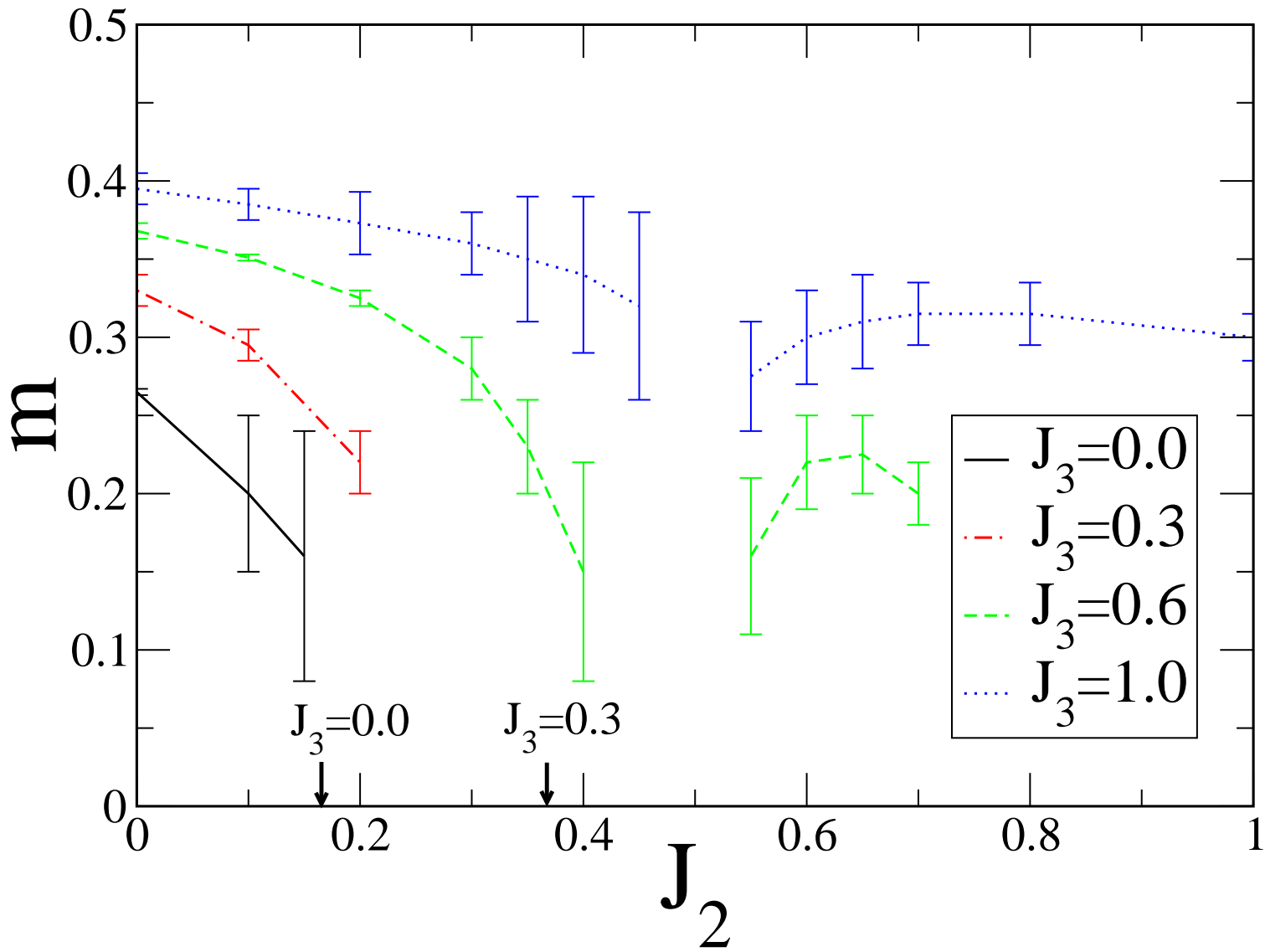


Figure 6 BG11636 24Aug2011

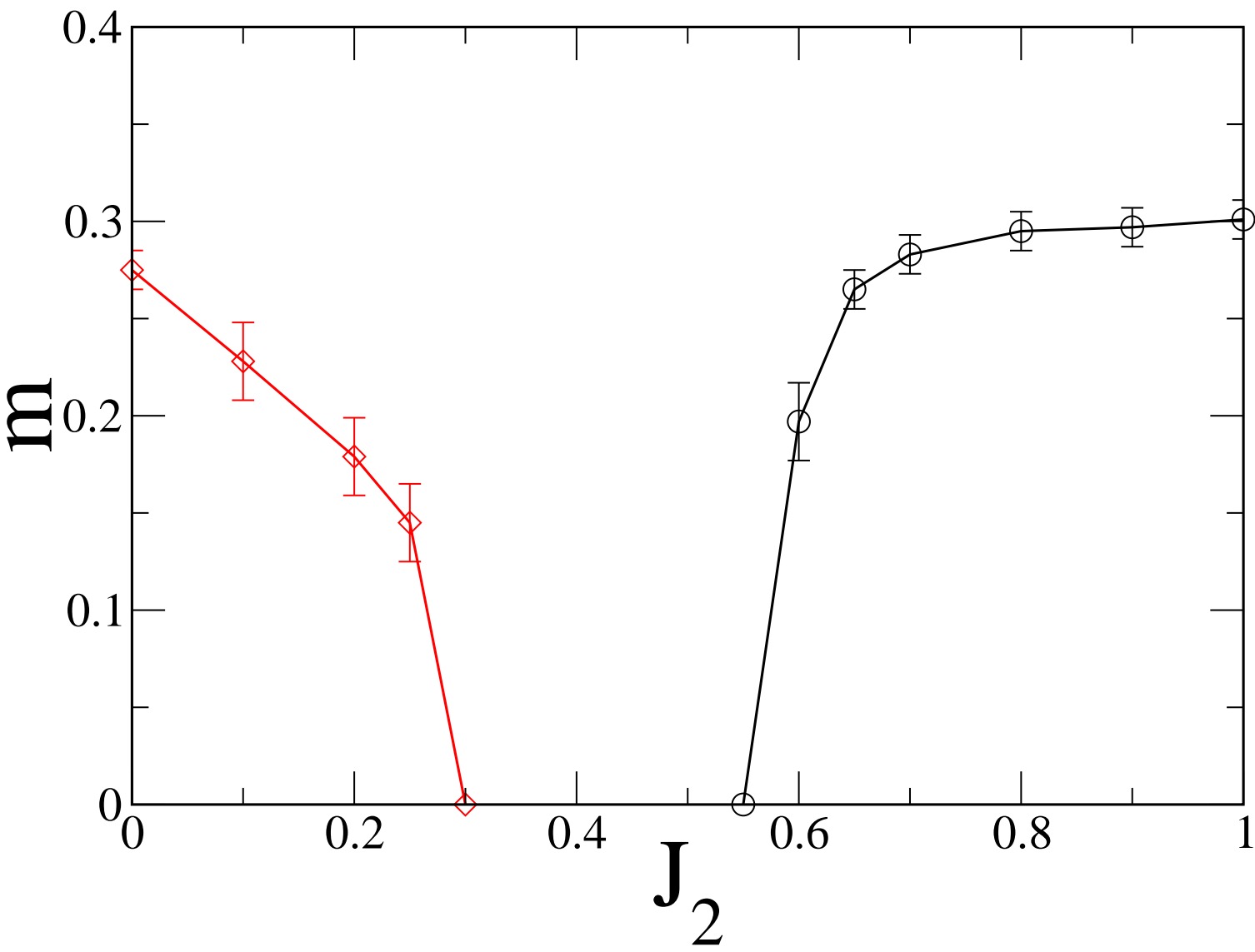


Figure 7 BG11636 24Aug2011

Figure 8 BG11636 24Aug2011

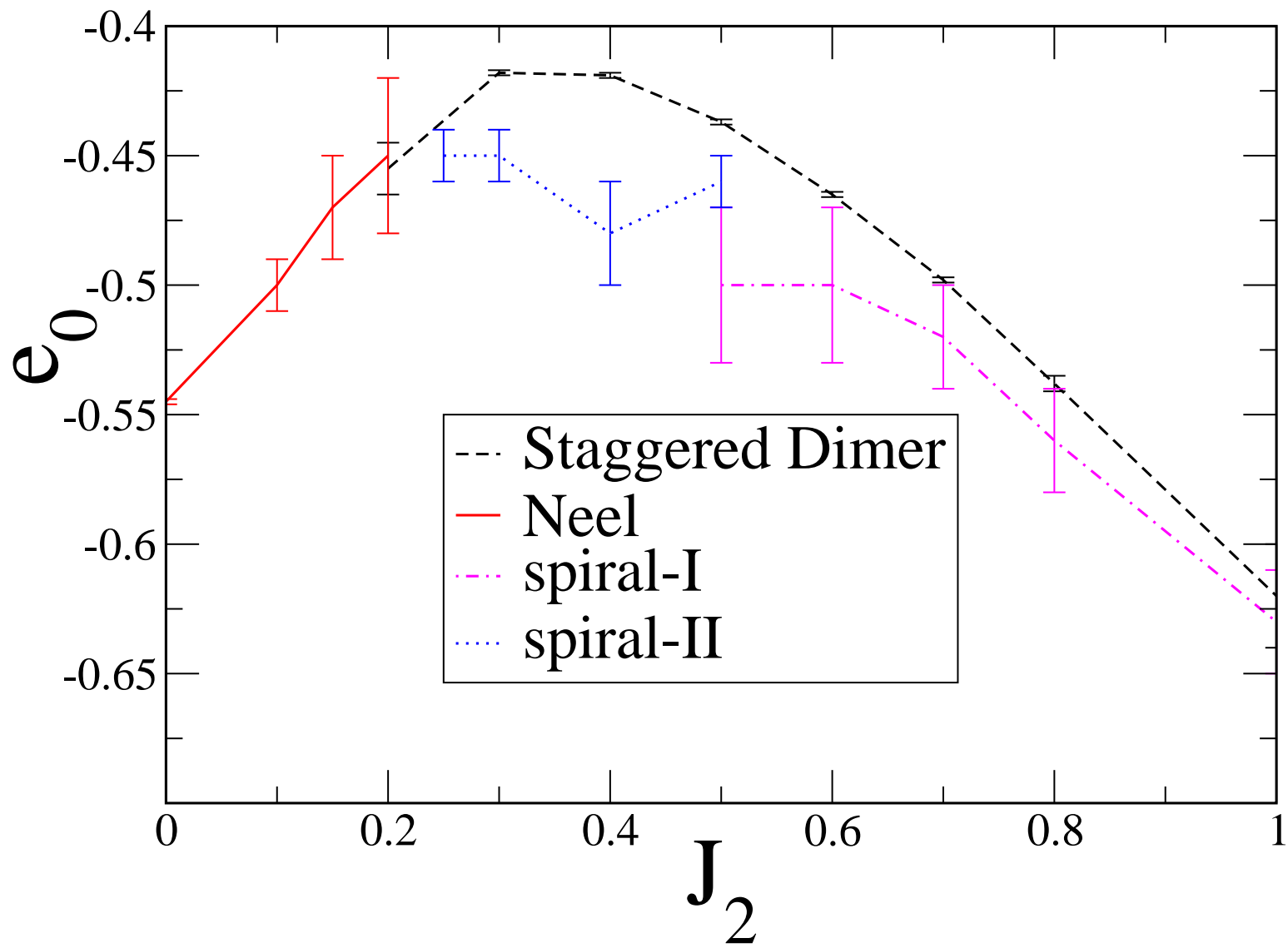


Figure 9 BG11636 24Aug2011

